

# The $\lambda_0 = 1.35$ cm H<sub>2</sub>O Maser Line: The Hyperfine Structure and Profile Asymmetry

D. A. Varshalovich\*, A. V. Ivanchik, and N. S. Babkovskaya

*Ioffe Physical-Technical Institute, ul. Politekhnikeskaya 26, St. Petersburg, 194021 Russia*

Received August 9, 2005

**Abstract**—The spectra of several H<sub>2</sub>O maser sources exhibit single  $\lambda_0 = 1.35$  cm maser lines with narrow asymmetric profiles. We consider the hyperfine structure of the line that corresponds to the transition between the rotational  $6_{16} \rightarrow 5_{23}$  levels of ortho-H<sub>2</sub>O molecules to account for the line asymmetry. Our numerical simulations of the maser line profile agree well with the observations if the hyperfine structure is taken into account.

PACS numbers : 98.58.Ec

DOI: 10.1134/S1063773706010051

Key words: *hyperfine structure, spectral profile, maser emission.*

## INTRODUCTION

Cosmic H<sub>2</sub>O maser emission at a wavelength of  $\lambda_0 = 1.35$  cm is observed from protoplanetary disks and jets in star-forming regions and, in several cases, from gas–dust accretion disks in the nuclei of certain active galaxies (Seyferts, liners, etc.). The observed maser lines often have complex profiles due to the superposition of several features from different subsources (see, e.g., Matveyenko 1981). However, in a number of cases, single, narrow (FWHM  $\sim 0.4$ – $0.8$  km s<sup>−1</sup>), and fairly intense lines with asymmetric profiles (the degree of asymmetry (see below) at half maximum is 1.1–1.3) are observed during maser flares; in general, the high-frequency line wing is flatter (Fig. 1).

The profile asymmetry of a single maser line is commonly explained either (1) by an asymmetry in the density and velocity distributions of the emitting H<sub>2</sub>O molecules in the maser source itself or (2) by a small radial-velocity shift of the resonantly absorbing H<sub>2</sub>O molecules on the line of sight between the source and the observer (Lekht *et al.* 2002; Silant'ev *et al.* 2002). Undoubtedly, both these factors can lead to a line profile asymmetry. However, to explain the profile asymmetry of a narrow maser line, the hyperfine splitting of the signal levels in the emitting molecules must primarily be taken into account. The goal of this paper is to consider the hyperfine (HF) structure of the  $\lambda_0 = 1.35$  cm H<sub>2</sub>O molecular line and to reveal the influence of this structure on the spectral profiles of the observed maser lines.

## THE HYPERFINE STRUCTURE OF SIGNAL LEVELS

The H<sub>2</sub>O molecules have two identical nuclei, two protons with the spins  $j_p = 1/2$ . Therefore, as with the H<sub>2</sub> molecules, two modifications of the water molecule exist, para-H<sub>2</sub>O and ortho-H<sub>2</sub>O, with a total nuclear spin  $I$  of 0 or 1 ( $\mathbf{I} = \mathbf{j}_p + \mathbf{j}_p$ ). Note that the nuclear spin of <sup>16</sup>O is zero.

The para-H<sub>2</sub>O levels ( $I = 0$ ) have no hyperfine structure, while all ortho-H<sub>2</sub>O levels ( $I = 1$ ) are split into three HF sublevels with  $F = J - 1, J,$  and  $J + 1$ , where  $J$  is the rotational angular momentum of the molecule, and  $\mathbf{F} = \mathbf{J} + \mathbf{I}$  is the total angular momentum of the system.

The  $\lambda_0 = 1.35$  cm maser line corresponds to the permitted E1 transition (i.e., to the electric dipole transition) between the rotational levels of the ortho-H<sub>2</sub>O molecules,  $J_{K_a K_c} = 6_{16} \rightarrow 5_{23}$  ( $K_a$  and  $K_c$  are the asymptotic quantum numbers that characterize the components of  $\mathbf{J}$  along the inner axes of the molecule). The excitation energies of these rotational levels are 447.253 and 446.511 cm<sup>−1</sup>, respectively, while their HF splitting does not exceed 10<sup>−5</sup> cm<sup>−1</sup>. Two factors are responsible for the hyperfine splitting of the ortho-H<sub>2</sub>O levels.

(A) The spin–rotational interaction, i.e., the interaction between the magnetic moments of the protons  $\boldsymbol{\mu}_p$  and the magnetic field  $\mathbf{H}_J$  generated by the molecular rotation in the region where the protons are located,

$$\Delta E_A = -2(\boldsymbol{\mu}_p \cdot \mathbf{H}_J). \quad (1)$$

\*E-mail: varsh@astro.ioffe.ru

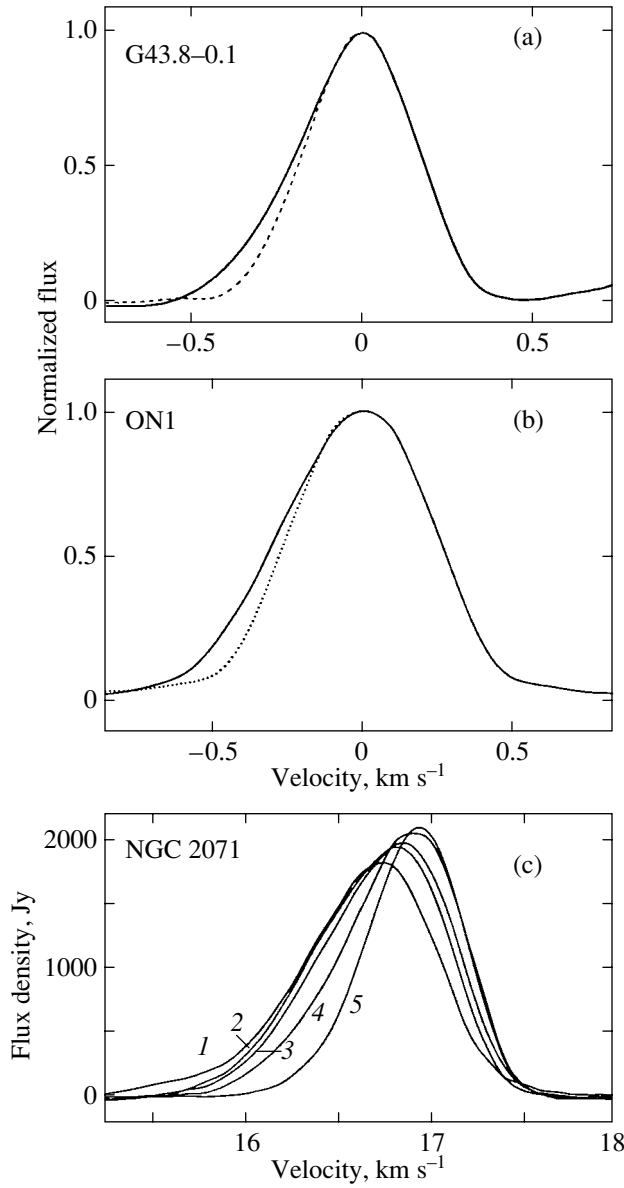


**Fig. 1.** Average normalized  $\lambda_0 = 1.35$  cm line profiles for the sources: (a) G43.8–01,  $v_{\text{LSR}} = 38.6$  km s $^{-1}$  during the flare of November 1981–May 1982; (b) ON1,  $v_{\text{LSR}} = 15.0$  km s $^{-1}$  during the flare of May 1994–December 1996; (c) the maser line profile for NGC 2071,  $v_{\text{LSR}} = 16.9$  km s $^{-1}$  on different days of the 1988–1989 flare.

(B) The spin–spin interaction, i.e., the interaction between the magnetic moments of the protons  $\mu_1$  and  $\mu_2$  averaged over various orientations of the rotating molecule in the  $J_{K_a K_c}$  state,

$$\Delta E_B = \left\langle \frac{(\mu_1 \cdot \mu_2)}{r_{12}^3} - 3 \frac{(\mu_1 \cdot \mathbf{r}_{12})(\mu_2 \cdot \mathbf{r}_{12})}{r_{12}^5} \right\rangle_J. \quad (2)$$

Here,  $\mathbf{r}_{12}$  is the vector that connects the protons (its equilibrium length is  $r_{12} = 1.514$  Å, and the zero-point oscillation amplitude is  $\delta r_{12} = 0.113$  Å).

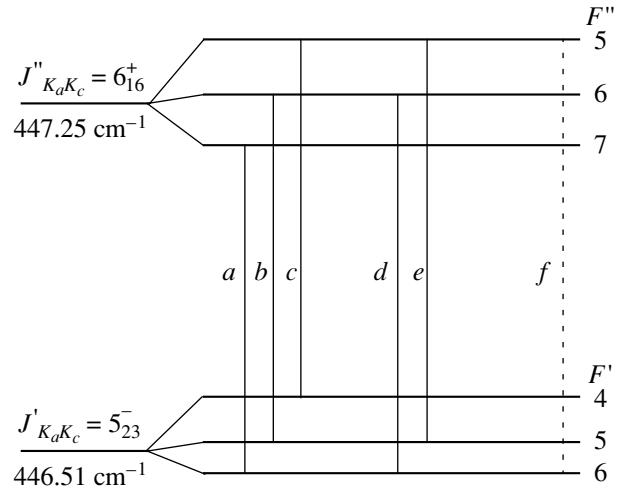


**Fig. 2.** Hyperfine splitting diagram for the H<sub>2</sub>O rotational  $J''_{K_a K_c} = 6_{16}^+$  and  $J'_{K_a K_c} = 5_{23}^-$  levels corresponding to the  $\lambda_0 = 1.35$  cm maser line.

According to (A) and (B), the hyperfine splitting as a function of  $F$  can be represented as the sum of two terms,

$$\Delta E_F(J) = A_J X(J, F) + B_J Y(J, F), \quad (3)$$

where

$$X(J, F) = F(F + 1) - J(J + 1) - I(I + 1), \quad (4)$$

$$Y(J, F) = X(X + 1) - \frac{4}{3} J(J + 1) I(I + 1). \quad (5)$$

We emphasize that the level “center of gravity” is not shifted in this splitting, since

$$\sum_F (2F + 1) \Delta E_F = 0. \quad (6)$$

The coefficients  $A_J$  and  $B_J$  in Eq. (3) depend not only on  $J$ , but also on  $K_a$  and  $K_c$ , since the H<sub>2</sub>O molecule is an asymmetric nonrigid rotator. As  $J$  increases, the angle  $\angle\text{HOH}$  and the OH bond lengths change appreciably; these changes in the molecular geometry depend on the orientation of the rotation axis.

Figure 2 shows the HF splitting diagram for the ortho-H<sub>2</sub>O rotational  $J''_{K_a K_c} = 6_{16}^+$  and  $J'_{K_a K_c} = 5_{23}^-$  levels that correspond to the  $\lambda_0 = 1.35$  cm maser line. The coefficients  $A_J$  and  $B_J$  can be determined from the laboratory frequency measurements of the HF components  $a, b, c, d, e$ , and  $f$  of this line (the notation is indicated in Fig. 2).

For the  $J''_{K_a K_c} = 6_{16}^+$  state,

$$\begin{cases} A'' = -[77(e - b) + 90(d - a)]/2184 \\ B'' = [7(e - b) - 6(d - a)]/2184. \end{cases}$$

**Table 1.** Shifts of the HF components in the  $\lambda_0 = 1.35$  cm ortho-H<sub>2</sub>O line [kHz] from laboratory measurements

HF component	Bluyssen <i>et al.</i> (1967) $\Delta\nu_B = \nu_B - \nu_B^0$	Kukulich (1969) $\Delta\nu_K = \nu_K - \nu_K^0$	Difference $\Delta\nu_B - \Delta\nu_K$
<i>a</i>	$-35.800 \pm 0.100$	$-35.856 \pm 0.047$	$0.056 \pm 0.055$
<i>b</i>	$-2.760 \pm 0.100$	$-2.790 \pm 0.048$	$0.030 \pm 0.055$
<i>c</i>	$40.400 \pm 0.100$	$40.512 \pm 0.045$	$-0.112 \pm 0.055$
<i>d</i>	$172.841 \pm 1.500$	$173.153 \pm 2.140$	$-0.313 \pm 1.310$
<i>e</i>	$218.041 \pm 1.200$	$217.854 \pm 2.150$	$0.186 \pm 1.230$
	$\nu_B^0 = 22\,235\,080.460$	$\nu_K^0 = 22\,235\,079.846$	0.614

For the  $J'_{K_a K_c} = 5_{23}$  state,

$$\begin{cases} A' = -[54(e - c) + 65(d - b)]/1320 \\ B' = [6(e - c) - 5(d - b)]/1320. \end{cases}$$

The frequency  $\nu^0$  corresponding to the  $6_{16}-5_{23}$  transition in the absence of HF splitting is defined by the relation

$$\nu^0 = (165a + 139b + 117c + 4d + 4e)/429.$$

Table 1 gives the frequency shifts of the HF line components,  $\Delta\nu = \nu - \nu^0$ , estimated from the laboratory measurements by Bluyssen *et al.* (1967) and Kukulich (1969). Comparison of the results obtained by these authors reveals a systematic frequency shift of  $\sim 0.6$  kHz. For the strong components *a*, *b*, and *c*, the measurement errors of the frequencies are smaller in Kukulich (1969); for the weak components *d* and *e*, they are smaller in Bluyssen *et al.* (1967). Therefore, we used the weighted mean frequencies from both papers corrected for their systematic shift  $\nu_B^0 - \nu_K^0 = 0.614$  kHz.

Table 2 gives our calculated coefficients  $A_J$  and  $B_J$  for the upper and lower signal levels,  $J''_{K_a K_c} = 6_{16}$  and  $J'_{K_a K_c} = 5_{23}$ , while Table 3 gives the corresponding hyperfine splitting of these levels.

The values of  $A''$  and  $A'$  allow us to estimate  $\langle H_J \rangle$ , the effective internal magnetic field generated by the molecular rotation  $\mathbf{J}$  at the proton locations,

$$\langle H_J \rangle = 0.470 A_J \sqrt{J(J+1)} [\text{G}]. \quad (7)$$

For the  $J'' = 6_{16}$  and  $J' = 5_{23}$  states, this field was found to be 49.9(2) and 40.9(2) G, respectively.

In the presence of an external magnetic field, apart from the HF splitting of the rotational molecular levels, Zeeman splitting of each of the HF sublevels  $F$  into  $2F + 1$  subcomponents differing only by  $M_F$ ,

the projection of  $\mathbf{F}$  onto the direction of the external magnetic field  $\mathbf{H}$ , arises,

$$\Delta E_{M_F}(JF) = -(\boldsymbol{\mu}_{JF} \cdot \mathbf{H}) = -\mu_{JF} H \cdot M_F / F. \quad (8)$$

To be able to determine this splitting and, accordingly, to estimate the external magnetic field, we must know the magnetic moments of each of the HF sublevels,

$$\boldsymbol{\mu}_{JF} = g_{JF} \mathbf{F}, \quad (9)$$

where

$$g_{JF} = \left( \frac{g_I + g_J}{2} \right) + \left( \frac{g_I - g_J}{2} \right) \times \frac{I(I+1) - J(J+1)}{F(F+1)}. \quad (10)$$

Here,  $g_I = 5.5857$  n.m., while  $g_{J''=6} = 0.6565$  n.m. and  $g_{J'=5} = 0.6959$  n.m. (Kukulich 1969). Table 4 gives  $\mu_{JF}$  for all HF components of the maser  $6_{16}$  and  $5_{23}$  levels. The values of  $\mu_{JF}$  are very low,  $\sim (5 \times 10^{-4} - 5 \times 10^{-3}) \mu_B$ . Therefore, no Zeeman splitting is observed in the overwhelming majority of known interstellar H<sub>2</sub>O masers. It will be comparable to the HF splitting of the rotational H<sub>2</sub>O levels only when the external magnetic field in the medium is strong enough,  $H \geq 10$  G. Therefore, below we may disregard it. However, when the polarization of maser emission is studied, the Zeeman splitting can be detected even at  $H \geq 0.05$  G (Fiebig and Gusten 1989).

**Table 2.** HF splitting parameters for the  $6_{16}$  and  $5_{23}$  ortho-H<sub>2</sub>O levels

$J'' = 6_{16}$	$J' = 5_{23}$
$A'' = -16.388$ kHz	$A' = -15.915$ kHz
$B'' = 0.1340$ kHz	$B' = 0.1412$ kHz

**Table 3.** Hyperfine splitting of the  $6_{16}$  and  $5_{23}$  ortho- $\text{H}_2\text{O}$  levels

$F''$	$\Delta E_{F''}(J'' = 6_{16})$ kHz	$F'$	$\Delta E_{F'}(J' = 5_{23})$ , kHz
5	$-14A'' + 70B'' = 238.812$	4	$-12A' + 52B' = 198.320$
6	$-2A'' - 110B'' = 18.036$	5	$-2A' - 78B' = 20.816$
7	$12A'' + 44B'' = -190.760$	6	$10A' + 30B' = -154.912$

### PARTIAL TRANSITION PROBABILITIES AND LINE STRENGTHS OF THE HYPERFINE COMPONENTS

In the absence of HF splitting, the probability of a spontaneous radiative transition, the Einstein coefficient  $A(J'' \rightarrow J')$ , is defined by the expression

$$(2J'' + 1)A(J'' \rightarrow J') \quad (11)$$

$$= \frac{4}{3}(2\pi\nu_{J''J'}/c)^3 S(J'' - J')/\hbar,$$

where  $S(J'' - J')$  is the so-called line strength, which is equal to the square of the reduced transition matrix element of the dipole moment operator,

$$S(J'' - J') = |\langle J'' || \hat{d} || J' \rangle|^2. \quad (12)$$

The probability of the  $J'' = 6_{16} \rightarrow J' = 5_{23}$  transition is  $A(J'' \rightarrow J') = 1.859 \times 10^{-9} \text{ s}^{-1}$ , and the corresponding line strength is  $S(J'' - J') = 1.888 D^2$  (Chandra *et al.* 1984).

In the presence of HF level splitting, the rotational  $J'' = 6_{16} \rightarrow J' = 5_{23}$  line splits into six components of different intensities,  $a, b, c, d, e,$  and  $f$  (Fig. 2). The partial line strengths for each of the HF component are defined by the expression

$$S(J''F'' - J'F') = (2F'' + 1)(2F' + 1) \quad (13)$$

$$\times \left\{ \begin{matrix} J'' & 1 & J' \\ F' & I & F'' \end{matrix} \right\}^2 S(J'' - J'),$$

**Table 4.** Magnetic moments of the  $\text{H}_2\text{O}$  molecule in the  $6_{16}$  and  $5_{23}$  states (in nuclear magnetons)

$F''$	$\mu_{J''F''}(6_{16})$	$F'$	$\mu_{J'F'}(5_{23})$
5	-0.8252	4	-1.1282
6	4.6432	5	4.2945
7	9.5269	6	9.0652

where  $\left\{ \begin{matrix} J'' & 1 & J' \\ F' & I & F'' \end{matrix} \right\}$  is the Wigner 6j-symbol (Varshalovich *et al.* 1988).

Table 5 gives the component frequencies  $\nu_{F''F'}$ , the relative line strengths  $S(J''F'' - J'F')/S(J'' - J')$ , and the corresponding probabilities of the partial transitions  $A(J''F'' \rightarrow J'F')/A(J'' \rightarrow J')$  between the HF components of the ortho- $\text{H}_2\text{O}$   $J'' = 6_{16}$  and  $J' = 5_{23}$  levels. We see from this table that only three of the six components,  $a, b,$  and  $c,$  are fairly intense. We emphasize that the total line strength for ortho- $\text{H}_2\text{O}$  increases by a factor of 3, proportionally to the statistical weight of the ortho-states, since

$$\sum_{F''F'} S(J''F'' - J'F') = (2I + 1)S(J'' - J'). \quad (14)$$

The probabilities of the corresponding partial transitions can be written as

$$A(J''F'' \rightarrow J'F') = (2J'' + 1)(2F' + 1) \quad (15)$$

$$\times \left\{ \begin{matrix} J'' & 1 & J' \\ F' & I & F'' \end{matrix} \right\}^2 A(J'' \rightarrow J').$$

Strictly speaking, Eq. (15) should be multiplied by the factor  $(\nu_{F''F'}/\nu_{J''J'})^3$ . However, this factor is equal to unity, to within  $10^{-6}$ – $10^{-5}$ . Therefore, despite the HF splitting, the total transition probabilities remain almost unchanged and identical for all HF sublevels  $F''$  (and their Zeeman subcomponents  $M''_F$ ), since

$$\sum_{F'} A(J''F'' \rightarrow J'F') = A(J'' \rightarrow J'), \quad (16)$$

$$\sum_{F'M'} A(J''F''M''_F \rightarrow J'F'M'_F) = A(J'' \rightarrow J'). \quad (17)$$

Thus, the lifetimes relative to the spontaneous radiative transitions are identical for all  $J''F''M''_F$  sub-states.

Note that the line strengths (13) reflect the actual intensities of the HF components only when the Zeeman sublevels of the HF components of the rotational

**Table 5.** Hyperfine components of the  $\lambda_0 = 1.35$  cm ortho-H<sub>2</sub>O line

Component	Transition $6_{16} - 5_{23}$ $F'' - F'$	Frequency $\nu_{F''F'}$ , kHz	Line strength $\frac{S(J''F'' - J'F')}{S(J'' - J')}$	Probability $\frac{A(J''F'' \rightarrow J'F')}{A(J'' \rightarrow J')}$
<i>a</i>	7–6	22 235 044.000	15/13	1.000 00
<i>b</i>	6–5	22 235 077.066	35/36	0.972 22
<i>c</i>	5–4	22 235 120.338	9/11	0.966 94
<i>d</i>	6–6	22 235 252.794	1/36	0.027 78
<i>e</i>	5–5	22 235 297.842	1/36	0.032 83
<i>f</i>	5–6	(22 235 473.570)	1/5148	0.000 23

molecular levels have equal populations, i.e., when the sublevel populations satisfy the relation

$$n_{JFM_F} = n_{JF}/(2F + 1). \quad (18)$$

Such a situation takes place in the case of isotropic pumping in the absence of selective HF sublevel excitation. This occurs fairly often, in the case of both collisional (Strelitsky 1980) and radiative (Deguchi 1981; Varshalovich *et al.* 1983) pumping. In general, the Zeeman components of the HF sublevels of the initial and final states can have different populations, with the HF line components being polarized. Such cases require a special analysis.

#### THE SPECTRAL PROFILE OF THE AMPLIFICATION COEFFICIENT

The amplification coefficient of a maser line (the negative absorption coefficient) in the absence of a HF structure of the signal levels for isotropic pumping is

$$\begin{aligned} \alpha_{J''J'}(\nu) &= \frac{\lambda_{J''J'}^2 (2J'' + 1) A(J'' \rightarrow J')}{8\pi \sqrt{\pi} \Delta\nu_D} \quad (19) \\ &\times N \left( \frac{n_{J''}}{2J'' + 1} - \frac{n_{J'}}{2J' + 1} \right) \phi_{J''J'}(\nu), \end{aligned}$$

where  $N$  is the number density of the working molecules and  $n_{J''}$  and  $n_{J'}$  are the relative signal level populations normalized in such a way that

$$\sum_J n_J = 1. \quad (20)$$

The spectral profile of the unsplit line,

$$\phi_{J''J'}(\nu) = \exp \left[ - \left( \frac{\nu - \nu_{J''J'}}{\Delta\nu_D} \right)^2 \right], \quad (21)$$

is normalized according to the condition

$$\int \phi_{J''J'}(\nu) d\nu = \sqrt{\pi} \Delta\nu_D. \quad (22)$$

Here,  $\Delta\nu_D$  is the Doppler line width,

$$\Delta\nu_D = \nu_{J''J'} v_T / c = v_T / \lambda_{J''J'}, \quad (23)$$

where  $v_T$  characterizes the spread in radial velocities of the working molecules. Given Eq. (11), the amplification coefficient (19) can be represented as

$$\begin{aligned} \alpha_{J''J'}(\nu) &= \frac{4}{3} \pi^{3/2} \frac{S(J'' - J')}{\hbar} \quad (24) \\ &\times \frac{N}{v_T} \left( \frac{n_{J''}}{2J'' + 1} - \frac{n_{J'}}{2J' + 1} \right) \phi_{J''J'}(\nu). \end{aligned}$$

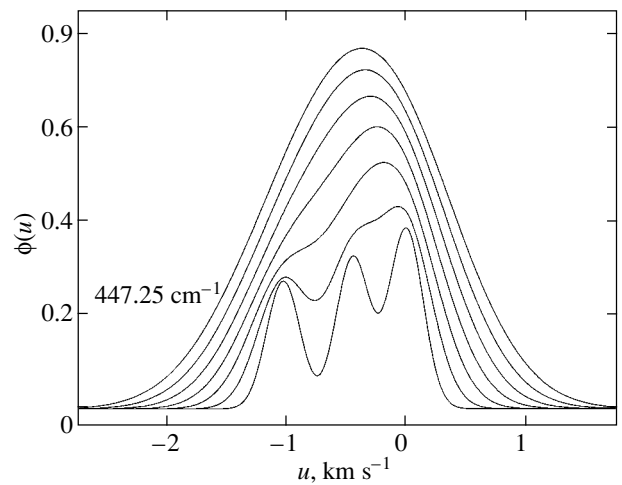


**Fig. 3.** Spectral profiles of the amplification coefficient for the maser line  $\phi(u)$  at various values of  $v_T$  that changes from 0.2 to 0.9 km s<sup>-1</sup> at 0.1 km s<sup>-1</sup> steps.

**Table 6.** Parameters of the profile of the amplification coefficient  $\phi(u)$  for the  $\lambda_0 = 1.35$  cm line

$v_T$ , km s <sup>-1</sup>	$u_0$ , km s <sup>-1</sup>	$(u_L + u_R)_{0.5}$ , km s <sup>-1</sup>	$(u_L/u_R)_{0.5}$	$(u_L + u_R)_{0.25}$ , km s <sup>-1</sup>	$(u_L/u_R)_{0.25}$
0.2	0.000	0.75	3.52	0.90	2.81
0.3	-0.071	1.39	3.70	1.65	3.08
0.4	-0.186	1.41	2.16	1.79	1.97
0.5	-0.243	1.46	1.68	1.93	1.60
0.6	-0.300	1.53	1.38	2.08	1.34
0.7	-0.343	1.62	1.20	2.23	1.20
0.8	-0.371	1.73	1.12	2.40	1.12
0.9	-0.386	1.84	1.08	2.56	1.08
1.0	-0.400	1.99	1.05	2.76	1.05

In the presence of HF signal level splitting, the amplification coefficient can be written as the sum of partial coefficients,

$$\begin{aligned} \alpha(\nu) &= \frac{N}{8\pi^{3/2}v_T} \sum_{F''F'} \lambda_{F''F'}^3 (2F'' + 1) \quad (25) \\ &\quad \times A(J''F'' \rightarrow J'F') \\ &\quad \times \left( \frac{n_{J''F''}}{2F'' + 1} - \frac{n_{J'F'}}{2F' + 1} \right) \phi_{F''F'}(\nu) \\ &= \frac{4}{3}\pi^{3/2} \frac{N}{v_T} \sum_{F''F'} \frac{S(J''F'' - J'F')}{\hbar} \\ &\quad \times \left( \frac{n_{J''F''}}{2F'' + 1} - \frac{n_{J'F'}}{2F' + 1} \right) \phi_{F''F'}(\nu). \end{aligned}$$

If there is no selective pumping of the HF components, then the HF sublevel populations can be expressed in terms of the total rotational level population  $n_J = \sum_F n_{JF}$ ,

$$\begin{aligned} \frac{n_{J''F''}}{(2F'' + 1)} &= \frac{n_{J''}}{(2J'' + 1)(2I + 1)}, \quad (26) \\ \frac{n_{J'F'}}{(2F' + 1)} &= \frac{n_{J'}}{(2J' + 1)(2I + 1)}. \end{aligned}$$

In this case, amplification coefficient (25) can be written in a form similar to (24),

$$\begin{aligned} \alpha_{HF}(\nu) &= \frac{4}{3}\pi^{3/2} \frac{S(J'' - J')}{\hbar} \frac{N}{v_T} \quad (27) \\ &\quad \times \left( \frac{n_{J''}}{2J'' + 1} - \frac{n_{J'}}{2J' + 1} \right) \phi_{HF}(\nu), \end{aligned}$$

where  $\phi_{HF}(\nu)$  is the total spectral line profile with HF splitting,

$$\phi_{HF}(\nu) = \frac{1}{(2I + 1)} \sum_{F''F'} \frac{S(J''F'' - J'F')}{S(J'' - J')} \phi_{F''F'}(\nu). \quad (28)$$

It is normalized to  $\sqrt{\pi}\Delta\nu_D$ , similar to (22). In the absence of HF splitting, when all  $\nu_{F''F'}$  are equal to  $\nu_{J''J'}$ , the function  $\phi_{HF}(\nu)$  transforms to  $\phi_{J''J'}(\nu)$ .

Radio astronomers commonly represent the profiles of a spectral line and the amplification coefficient as a function of the relative velocity  $u$ :

$$u = -c \left( \frac{\nu - \nu_0}{\nu_0} \right). \quad (29)$$

In the presence of HF components, the spectral profile depends significantly on  $\Delta\nu_D$ , i.e., on the parameter  $v_T$ . In the case of interest, the narrow emission lines most likely originate in a medium with a kinetic temperature  $T_{\text{kin}} \sim 100$ – $1000$  K at a low turbulence level. For water molecules, this corresponds to  $v_T \sim 0.3$ – $1.0$  km s<sup>-1</sup>. In this case, for the H<sub>2</sub>O 1.35-cm maser line, the total profile of the amplification coefficient can be written as the superposition of three profiles,

$$\begin{aligned} \phi(u) &= ae^{-\left(\frac{u-u_a}{v_T}\right)^2} \quad (30) \\ &\quad + be^{-\left(\frac{u-u_b}{v_T}\right)^2} + ce^{-\left(\frac{u-u_c}{v_T}\right)^2}, \end{aligned}$$

where  $a = 0.3919$ ,  $b = 0.3302$ ,  $c = 0.2779$  and  $u_a = 0$ ,  $u_b = -0.4458$ , and  $u_c = -1.0293$  km s<sup>-1</sup>. The

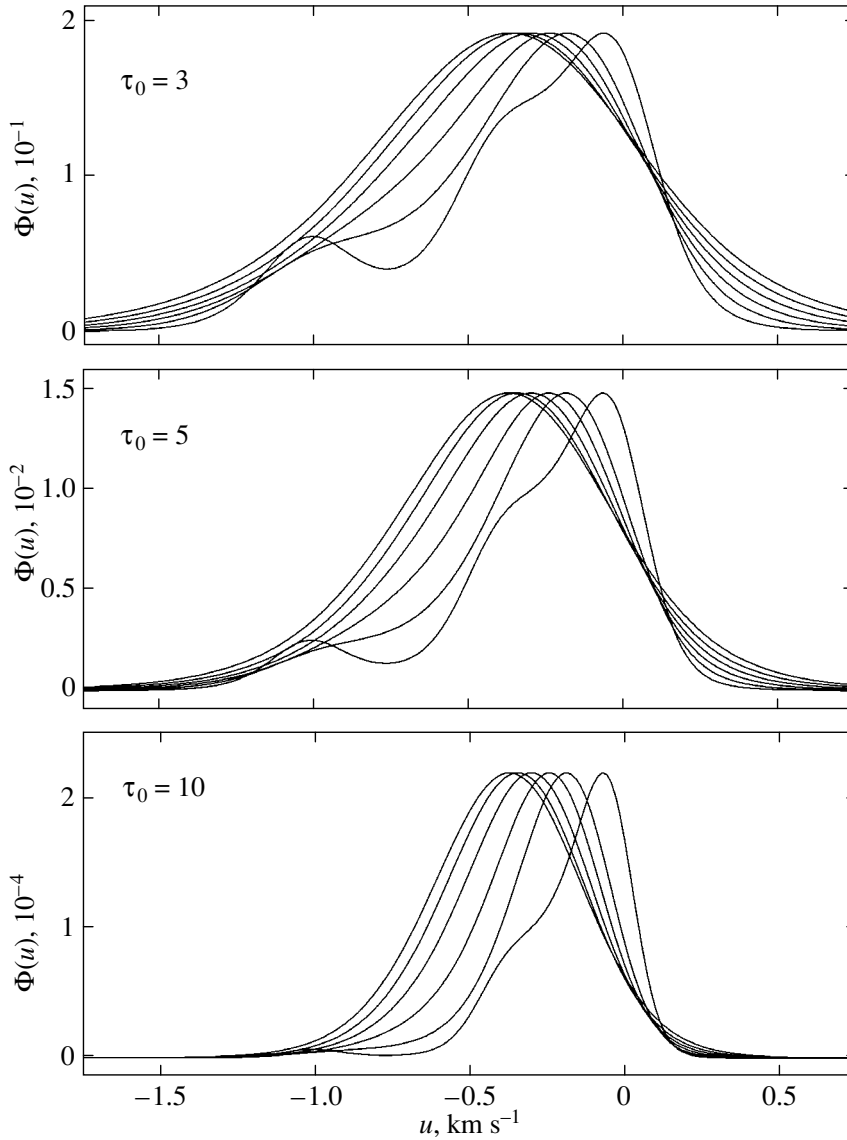


Fig. 4. Maser line profiles  $\Phi(u)$  as a function of  $v_T$  at fixed  $\tau_0$ ; the profiles correspond to  $v_T$  from 0.3 to 0.8 km s<sup>-1</sup> at 0.1 km s<sup>-1</sup> steps.

contribution from the three remaining HF components ( $u_d = -2.82$ ,  $u_e = -3.42$ ,  $u_f = -5.79$  km s<sup>-1</sup>) to the total profile near the maximum is  $3 \times 10^{-6}$ , since the corresponding weighting coefficients are small,  $d = e = 0.00926$  and  $f = 0.00006$ .

Figure 3 presents the functions  $\phi(u)$  for several values of the parameter  $v_T$ :

—at  $v_T < 0.27$  km s<sup>-1</sup>, the profile  $\phi(u)$  has three maxima corresponding to  $u_a$ ,  $u_b$ , and  $u_c$ ;

—at  $0.27 < v_T < 0.35$  km s<sup>-1</sup>, the components  $u_a$  and  $u_b$  merge into a single line, while the component  $u_c$  remains separate; and

—at  $v_T > 0.35$  km s<sup>-1</sup>, all three components merge into a single broad asymmetric profile.

Since the profile has a multicomponent structure, it is appropriate to characterize the profile not only by the values of the parameters at half maximum, at  $\xi = 0.5$ , but also at other  $\xi$  values. The asymmetry of the profile  $\phi(u)$  can be defined as the ratio of the half-widths of the left and right wings  $(u_L/u_R)_\xi$  at the  $\xi$  level, while the full width of the profile can be defined as the sum of these half-widths  $(u_L + u_R)_\xi$ .

Table 6 gives the parameters of the function  $\phi(u)$ , more specifically, the shifts of the line maximum  $u_0$ , the full widths  $(u_L + u_R)_{0.5}$  and  $(u_L + u_R)_{0.25}$ , and the corresponding asymmetry coefficients  $(u_L/u_R)_{0.5}$  and  $(u_L/u_R)_{0.25}$ . As  $v_T$  increases, the profile maximum monotonically shifts and the profile becomes broader

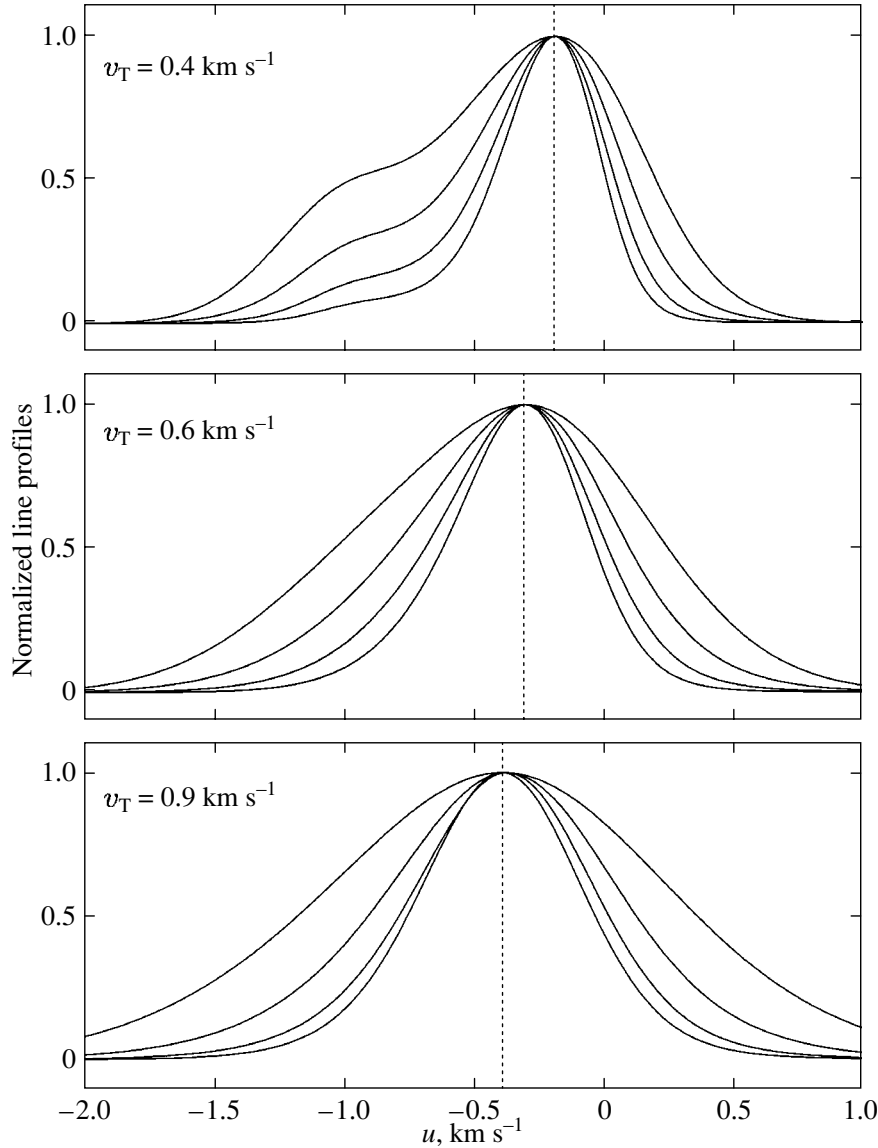


**Fig. 5.** Normalized maser line profiles  $\Phi(u)/\Phi(u_0)$  as a function of  $\tau_0$  at fixed  $v_T$ ; the profiles correspond to  $\tau_0 = 1, 3, 5,$  and  $7$ .

and less asymmetric. In this case, the values of  $\phi(u_0)$  increase, but the ratios  $\phi(u_0)/v_T$  decrease.

### THE MASER LINE PROFILE

In an active medium with an amplification coefficient  $\alpha_{HF}(\nu)$ , the intensity of a traveling wave that traversed a distance  $L$  is defined by the expression

$$\mathcal{I}_\nu(\tau_\nu) = \mathcal{I}_\nu(0)e^{\tau_\nu} + \int_0^{\tau_\nu} \mathcal{S}_\nu(\tau'_\nu) e^{\tau'_\nu} d\tau'_\nu. \quad (31)$$

Here,  $\mathcal{I}_\nu(0)$  is the intensity of the incoming radiation;  $\tau_\nu$  is the optical depth of the medium at frequency  $\nu$ ,

$$\tau_\nu = \int_0^L \alpha_{HF}(\nu, z) dz; \quad (32)$$

and  $\mathcal{S}_\nu(\tau'_\nu)$  is the source function, which is defined as the ratio of the emissivity of the medium and the amplification coefficient at frequency  $\nu$  at point  $\tau'_\nu$ .

The relative population of signal levels is commonly characterized by their excitation temperature  $T_{\text{ex}}$ , which is defined by the relation

$$\frac{n_{J''}}{n_{J'}} = \frac{2J'' + 1}{2J' + 1} \exp \left[ -\frac{\varepsilon_{J''J'}}{kT_{\text{ex}}(J''J')} \right]. \quad (33)$$

$T_{\text{ex}} < 0$  corresponds to an inverted level population. In this case, the source function for the maser emission is

$$\mathcal{S}_\nu = -\frac{h\nu_{J''J'}^3}{2c^2} \coth \frac{h\nu_{J''J'}}{2kT_{\text{ex}}(J''J')} \simeq -\frac{kT_{\text{ex}}(J''J')}{\lambda_{J''J'}^2}. \quad (34)$$

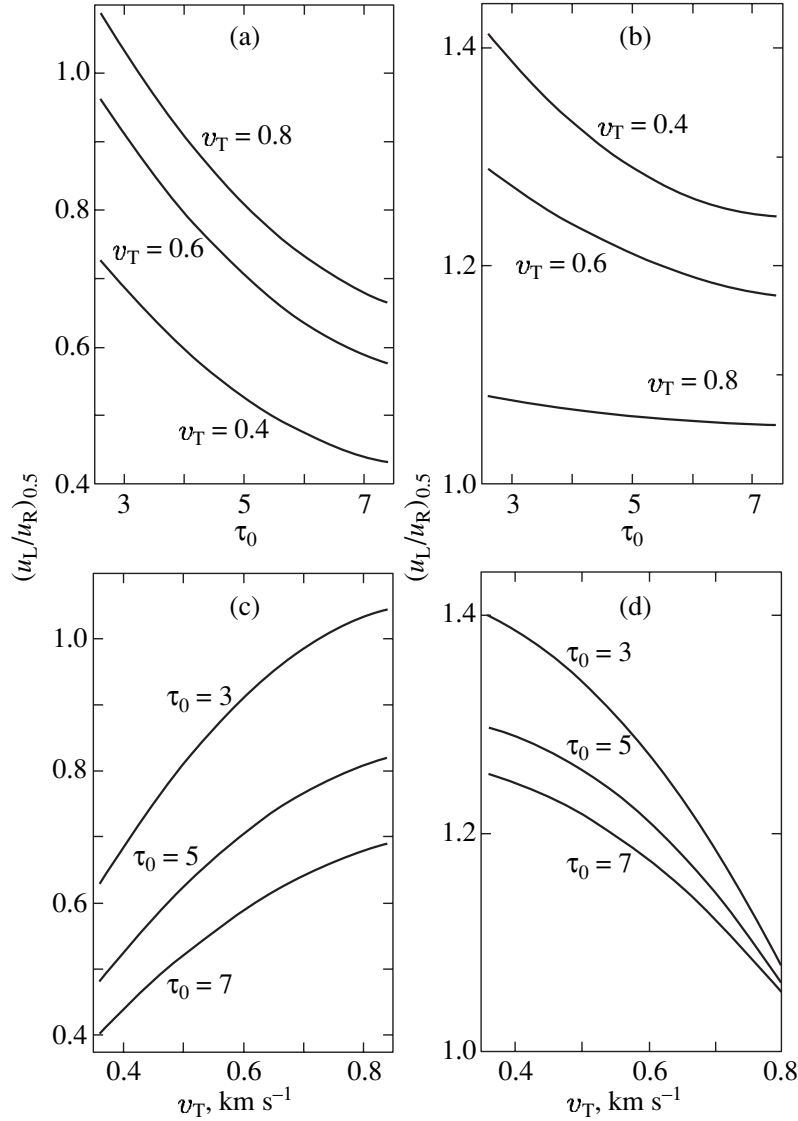


**Fig. 6.** Maser line width  $(u_L + u_R)_{0.5}$  and degree of asymmetry  $(u_L/u_R)_{0.5}$  as functions of  $\tau_0$  and  $v_T$ .

To find out how the HF structure of the signal levels affects the profile asymmetry of the observed maser line, we should exclude all of the other factors (except the HF structure) that can influence the asymmetry of the spectral profile, more specifically, the difference between the profiles of the emission and absorption coefficients and the velocity gradients in the emitting and absorbing matter. Therefore, we consider the intrinsic emission from a homogeneous unsaturated medium, i.e., the case of  $\mathcal{I}_\nu(0) = 0$  and  $\mathcal{S}_\nu(\tau'_\nu) = \text{const}$ . In this case, the line intensity is

$$\mathcal{I}_\nu(\tau_\nu) = \mathcal{S}_\nu(e^{\tau_\nu} - 1). \quad (35)$$

For the maser line, by our definitions,  $\mathcal{S}_\nu > 0$  and  $\tau_\nu > 0$ . The optical depth of the medium in terms of the relative velocity  $u$  (see (29)) is  $\tau_u = \tau_0(\phi(u)/\phi(u_0))$ ,

and its value at the line maximum is

$$\begin{aligned} \tau_0 = & -\frac{4}{3}\pi^{3/2}S(J'' - J') \left( \frac{NL}{\hbar v_T} \right) \quad (36) \\ & \times \frac{n_{J''}}{2J'' + 1} \frac{\hbar \nu_{J''J'}}{kT_{\text{ex}}(J''J')} \phi(u_0). \end{aligned}$$

The spectral profile of the maser line,

$$\Phi(u) \equiv \exp(\tau_u) - 1, \quad (37)$$

is naturally determined by the profile of the amplification coefficient  $\phi(u)$ . The line intensity maximum  $\Phi(u_0)$  corresponds to the same velocity  $u_0$  as the maximum of the amplification coefficient  $\phi(u_0)$ . At the same time, the intensity of the line emission  $\Phi(u)$  at the  $\eta$  level of its maximum value  $\Phi(u_0)$  corresponds

to the same velocity  $u$  at which the relative amplification coefficient  $\phi(u)/\phi(u_0)$  is equal to  $\xi$ ,

$$\xi = \frac{1}{\tau_0} \ln[1 + \eta(e^{\tau_0} - 1)]. \quad (38)$$

At  $\tau_0 \gg 1$ , the full width and asymmetry of the maser line  $\Phi(u)$  at half maximum,  $(u_L + u_R)_\eta$  and  $(u_L/u_R)_\eta$  at  $\eta = 0.5$ , are equal to the full width  $(u_L + u_R)_\xi$  and asymmetry  $(u_L/u_R)_\xi$  of the function  $\phi(u)$  at the  $\xi = 1 - \ln 2/\tau_0$  level of its maximum.

Thus, the maser line profile  $\Phi(u)$  is a function of two parameters,  $v_T$  and  $\tau_0$ . The profile  $\Phi(u)$  shifts and broadens without changing its height with increasing  $v_T$  and at fixed  $\tau_0$ ; the line asymmetry decreases. The function  $\Phi(u)$  increases exponentially, its profile narrows sharply without shifting, and its asymmetry decreases with increasing  $\tau_0$  and under fixed  $v_T$ . The line profiles  $\Phi(u)$  are shown in explicit form in Figs. 4 and 5 for various  $v_T$  and  $\tau_0$ . The corresponding dependences of the full width of the maser line,  $(u_L + u_R)_{0.5}$ , and the degree of its asymmetry,  $(u_L/u_R)_{0.5}$ , are shown in Fig. 6. Varying the parameters  $v_T$  and  $\tau_0$ , we can reproduce the profiles of the observed maser lines (Fig. 1). Of course, it is appropriate to make a detailed digital comparison of the profiles separately for each of the spectra obtained rather than for the averaged profiles. This will make it possible to trace the dynamics of the maser flare.

## CONCLUSIONS

Allowance for the hyperfine structure of the  $\lambda_0 = 1.35$ -cm maser line of  $\text{H}_2\text{O}$  molecules naturally explains the rise of the high-frequency line wing ( $u_L > u_R$ ), the observed degree of asymmetry  $(u_L/u_R) = 1.1$ – $1.3$  and the observed width of the line, and the line shift by  $0.1$ – $0.3 \text{ km s}^{-1}$  observed in several cases. There is no need to assume the existence of velocity gradients of the emitting or absorbing molecules, although, undoubtedly, these gradients can additionally affect the observed line parameters.

## ACKNOWLEDGMENTS

This work was supported by the ‘‘Program for Support of Leading Scientific Schools’’ (no. NSh-1115.2003.2), the Russian Foundation for Basic Research (project no. 05-02-17065-a) and the ‘‘Non-stationary Phenomena in Astronomy’’ and ‘‘Extended Objects in the Universe’’ programs of the Russian Academy of Sciences.

## REFERENCES

1. H. Bluysen, A. Dymanus, and J. Verhoeven, *Phys. Lett.* **24A**, 482 (1967).
2. S. Chandra, D. A. Varshalovich, and W. H. Kegel, *Astron. Astrophys., Suppl. Ser.* **55**, 51 (1984).
3. S. Deguchi, *Astrophys. J.* **249**, 145 (1981).
4. D. Fiebig and R. Gusten, *Astron. Astrophys.* **214**, 333 (1989).
5. S. Kukolich, *J. Chem. Phys.* **50**, 3751 (1969).
6. E. E. Lekht, N. A. Silant’ev, J. E. Mendosa-Torres, and A. M. Tolmachev, *Pis’ma Astron. Zh.* **28**, 106 (2002) [*Astron. Lett.* **28**, 89 (2002)].
7. L. I. Matveyenko, *Astrophys. Space Phys. Rev.* **1**, 83 (1981).
8. N. A. Silant’ev, E. E. Lekht, J. E. Mendosa-Torres, and A. M. Tolmachev, *Pis’ma Astron. Zh.* **28**, 253 (2002) [*Astron. Lett.* **28**, 217 (2002)].
9. V. S. Strel’nitsky, *Pis’ma Astron. Zh.* **6**, 354 (1980) [*Sov. Astron. Lett.* **6**, 196 (1980)].
10. D. A. Varshalovich, W. H. Kegel, and S. Chandra, *Pis’ma Astron. Zh.* **9**, 395 (1983) [*Sov. Astron. Lett.* **9**, 209 (1983)].
11. D. A. Varshalovich, A. N. Moskalev, and V. K. Kher-sonskii, *Quantum Theory of Angular Momentum* (Nauka, Leningrad, 1975; World Sci., Singapore, 1988).

*Translated by V. Astakhov*